THE JOURNAL OF PHYSICAL CHEMISTRY B

Article

pubs.acs.org/JPCB

# Interaction of Presequence with Human Translocase of the Inner Membrane of Mitochondria Tim50

Yongqiang Zhang,[†,‡] Honghua Deng,[†] Qing Zhao,[†] and Shu Jie Li*[,†]

[†]The Key Laboratory of Bioactive Materials, Ministry of Education, School of Physics Science, Nankai University, Tianjin 300071, P. R. China

[‡]Basic Department, Bengbu Automobile Sergeant School of the People's Liberation Army, Bengbu 233011, P. R. China

**ABSTRACT:** The preprotein translocase of the inner membrane of mitochondria (TIM23 complex) is the main entry gate for proteins of the matrix and the inner membrane. Tim50 is a major receptor for transporting the precursor protein across the mitochondrial inner membrane in the TIM23 complex. However, the interaction of prequence peptide with Tim50 is not well-known. Here, we investigated in vitro the interaction of presequence peptide with the intermembrane space domain of Tim50 ($Tim50_{IMS}$) by micro-Raman and fluorescence spectra. The fluorescence quenching revealed that the interaction between $Tim50_{IMS}$ and presequence peptide is mainly electrostatic interaction, and the distances between $Tim50_{IMS}$ and presequence peptides are estimated by fluorescence resonance energy transfer. Micro-Raman spectra showed that presequence peptides induce a more compact conformation of $Tim50_{IMS}$, and synchronous fluorescence showed that the tyrosine or tryptophan fluorescence quenching molar ratio of presequence peptide to $Tim50_{IMS}$ is less than 3.

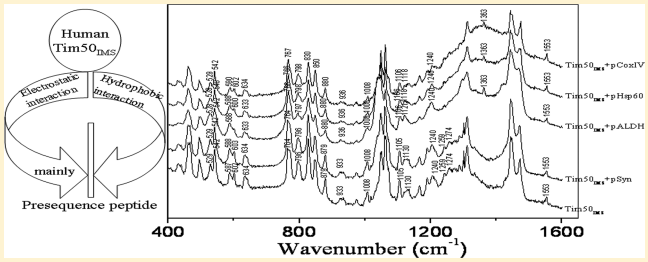


## 1. INTRODUCTION

The vast majority of mitochondrial proteins are synthesized as precursor proteins on cytosolic ribosomes, subsequently imported into mitochondria.[1−3] The importing process is completed through the membrane-protein complexes called translocators in the outer and inner membranes and soluble factors in the cytosol, intermembrane space (IMS), and matrix.[4] The TOM40 complex located in the outer mitochondrial membrane functions as a common entry gate for most mitochondrial proteins.[5] After passing through the TOM40 complex, the precursors mainly use four different pathways to the mitochondrial subcompartments.[4−6] The four pathways are as follows: the carrier pathway to the inner membrane by the TIM22 complex in the inner membrane, which is required for the insertion of presequence-less polytopic membrane proteins including mitochondrial carrier proteins into the inner membrane; the presequence pathway to the matrix and inner membrane by the TIM23 complex in the inner membrane, which mediates the translocation of mitochondrial precursor proteins with an N-terminal cleavable presequence across and insertion into the inner membrane; the transport pathways of outer membrane proteins by the TOB/SAM complex in the outer membrane, which mediates the assembly of $\beta$-barrel membrane proteins into the outer membrane; and the oxidative folding pathway of the IMS by Tim40/Mia40 and Erv1, which constitute a disulfide relay system in the IMS to facilitate import and oxidative folding of mainly small soluble proteins in the IMS.[4−6] The TIM23 complex, which mediates the import of essentially all matrix proteins and a large number of inner membrane proteins, contains 10 subunits: Tim50, Tim23, Tim17, Tim44, Tim14, Tim16, Tim21, Pam17, mtHsp70, and Mge1.[7] The core complex comprises the three subunits Tim23, Tim17, and Tim50. Tim44 can be viewed as a coordinating subunit at the matrix side of the TIM23 complex. Tim14 is anchored in the inner membrane with a single transmembrane domain exposing its conserved J domain into the matrix and a less well-defined N-terminal segment into IMS. The latter has been proposed to mediate the direct interaction of Tim14 with Tim17. Tim16 is a matrix protein peripherally attached to the inner membrane, and it forms an unusually stable subcomplex of the TIM23 translocase with Tim14. Matrix heat shock protein 70 (mtHsp70) is the ATP-hydrolyzing subunit of the complex. Mge1 is a soluble matrix protein that serves as a nucleotide exchange factor of mtHsp70. Tim21 and Pam17 are not essential for cell viability.[7]

The mitochondrial targeting signal is contained within precursor proteins, often in the form of an N-terminal presequence, which typically consists of 15−40 amino-acid residues, with an abundance of positively charged residues, and tends to form an amphiphilic helical conformation.[8] Tim50, which is the first component to receive the translocating precursor protein from the TOM40 complex at the inner membrane,[9] recognizes the presequence part of the precursors,[10] and the IMS domain of Tim50 ($Tim50_{IMS}$) induces the Tim23 channel to close, while presequences overcome this effect and activate the channel for translocation.[11] It was

**Received:** November 10, 2011
**Revised:** February 13, 2012
**Published:** February 15, 2012

   dx.doi.org/10.1021/jp2108279 | J. Phys. Chem. B 2012, 116, 2990−2998

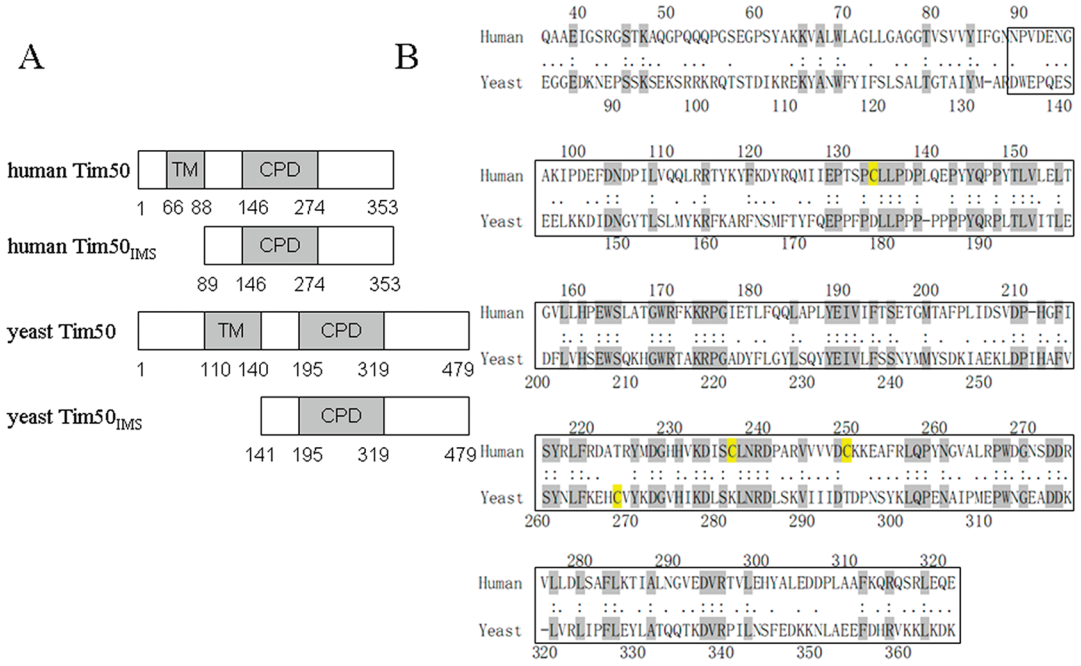


**Figure 1.** (A) Domain structures of human Tim50, human $Tim50_{IMS}$, yeast Tim50, yeast $Tim50_{IMS}$ are represented by bar diagrams. The numbers indicate the boundaries of these domains. (B) Amide acid sequence similarity alignments of the human Tim50 and yeast Tim50 in A; the amide acid sequence similarity alignments of human $Tim50_{IMS}$ and yeast $Tim50_{IMS}$ are marked by a pane. Human Tim50 and yeast Tim50 has a similarity of 31.4%, and the IMS domain has a similarity of 35.7%.

reported that the interaction between the presequence peptide and Tim50 is hydrophobic interaction.[12−14] Qian et al.[15] recently reported the crystal structure of the IMS domain of yeast Tim50 that forms a monomer and consists of five $\alpha$-helices and nine $\beta$-strands. A $\beta$-hairpin protruding out of the Tim50 molecular surface represents the largest conserved area on the Tim50. Additionally, a large groove, which contains several exposed negatively charged residues, may be ideally suited as a binding site for positively charged presequences/preproteins.

Human Tim50 is composed of 353 amino acids, which spans the inner membrane with a single transmembrane segment (66−88 residues) and exposes a large hydrophilic domain[16] in the IMS (89−353 residues) containing C-terminal domain (CTD)-like phosphatase domain (CPD) (146−274 residues) (See Figure 1).[9] Human Tim50 and yeast Tim50 have an amide acid sequence similarity of 31.4%, and their IMS domains have a similarity of 35.7%.[9] To fully understand the biological functions of TIM23 complex at molecular basis, detailed information about the interaction between Tim50 and presequence is necessary. In the present study, the interactions of human $Tim50_{IMS}$ with presequence peptides were investigated by micro-Raman and fluorescence spectra. Our results showed that the presequence peptides interact with $Tim50_{IMS}$ mainly through electrostatic interaction, and the interaction induces a more compact conformation of $Tim50_{IMS}$.

## 2. MATERIALS AND METHODS

**2.1. Protein Expression and Purification.** The expression and purification of the protein was as described in our previous work.[17] Briefly, *Escherichia coli* strain BL21 (DE3) transformed with pIMS-$Tim50_{IMS}$ was grown to an absorbance of 1.0 at 600 nm ($A_{600}$) in LB medium in the presence of 100 $\mu$g $mL^{-1}$ ampicillin at 21 °C, and induced with 0.5 mM isopropyl-$\beta$-D-thiogalactopyranoside (IPTG) at 14 °C for 24 h. The protein was purified by a Glutathione-Sepharose 4B (GE Healthcare) column, an ion exchange HiTrap Q FF column (GE Healthcare), and a Superdex 75 16/60 gel filtration column (GE Healthcare). The concentration of the protein was determined by extinction coefficient 38 515 $M^{-1}\cdot cm^{-1}$.[18]

**2.2. Presequence Peptide.** pCoxIV (MLATRVFSLVGKRAISTSVCVR) represents the presequence of human cytochrome c oxidase subunit IV.[19] pHsp60 (MLRLPTVFRQMRPVSRVLA PHLTRA) represents the presequence of human heat shock protein 60.[13] pALDH (MLRAAARFGPRLGRRLL) represents the presequence of human aldehyde dehydrogenase.[14] pSyn (KTRSRTRMVISVGASFVALSLV) represents the peptide with the same amino-acid composition as the pCox IV but with a scrambled sequence. pCoxIV was synthetized by Sigma, and pHsp60, pALDH, and pSyn were synthetized by Ketai Co. (Shanghai, China)

**2.3. Fluorescence Quenching.** Fluorescent quenching experiments were carried out on an Edinburgh fluorescence spectrometer (NIR 301/2) at 25 and 35 °C. Titration was done by adding small volumes of concentrated pCoxIV (420 $\mu$M), pALDH (320 $\mu$M), pHsp60 (320 $\mu$M), and pSyn (320 $\mu$M) to a cuvette containing 2 mL of a 1.6 $\mu$M solution of $Tim50_{IMS}$ in 10 mM sodium phosphate buffer (pH 7.4) with 0.15 M NaCl and 1.5 M NaCl, respectively, allowing the mixture to equilibrate for 5 min. The volume of added presequence peptide never exceeded 5% of the total volume. The excitation wavelength was set at 295 nm with a slit width of 5 nm, and the fluorescence emission spectra were scanned from 300 to 500 nm with a slit width of 5 nm. The spectra of samples were corrected by subtracting the corresponding spectra of buffers in the absence of protein.

Fluorescence quenching data in the presence of the presequence peptide were fitted to the Stern−Volmer equation


dx.doi.org/10.1021/jp2108279 | J. Phys. Chem. B 2012, 116, 2990−2998

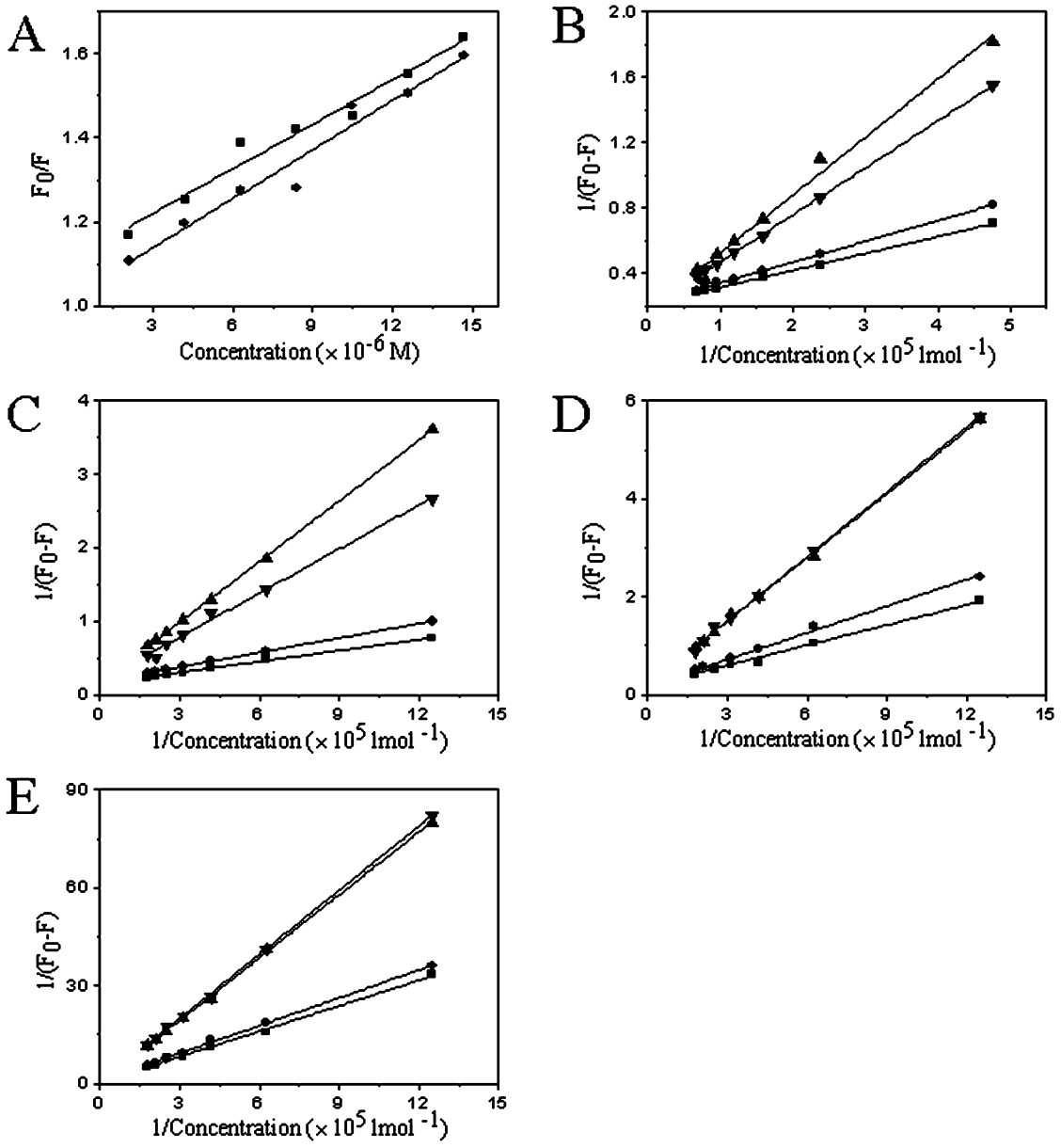


**Figure 2.** (A) the Stern−Volmer plots for the fluorescence quenching of $Tim50_{IMS}$ by pCoxIV at 25 and 35 °C. The $K_{SV}$ values were obtained from the slope of a linear dependence of $F_0/F$ versus the free concentration of pCoxIV. (B) The static quenching plots for the fluorescence quenching of $Tim50_{IMS}$ by pCoxIV. (C) The static quenching plots for the fluorescence quenching of $Tim50_{IMS}$ by pALDH. (D) The static quenching plots for the fluorescence quenching of $Tim50_{IMS}$ by pHsp60. (E) The static quenching plots for the fluorescence quenching of $Tim50_{IMS}$ by pSyn. The concentration of $Tim50_{IMS}$ was 0.05 mg $mL^{-1}$ (1.6 $\mu$M). ■, 25 °C, 0.15 M NaCl; ●, 35 °C, 0.15 M NaCl; ▲, 25 °C, 1.5 M NaCl; ▼, 35 °C, 1.5 M NaCl.

and the static quenching equation. The Stern−Volmer equation[20] is

$$F_0/F = 1 + K_q\tau_0[Q] = 1 + K_{SV}[Q] \quad (1)$$

and the static quenching equation is

$$1/(F_0 - F) = 1/F_0 + 1/(K_A F_0[Q]) = 1/F_0 + K_D/(F_0[Q]) \quad (2)$$

where $F_0$ and $F$ are the fluorescence intensities in the absence and presence of the presequence peptide, respectively. $K_q$ is the quenching rate constant of the biomolecule; $\tau_0$ is the average lifetime of the molecule without quencher; [Q] is the free concentration of the presequence peptide; $K_{SV}$ is the dynamic quenching constant; $K_A$ is the formation constant; and $K_D$ is the dissociation constant.

In order to determinate the interaction characteristics between $Tim50_{IMS}$ and the presequence peptide, such as hydrogen bond, van der Waals force, and electrostatic and hydrophobic interaction, the following equations were used:

$$\ln K_A = -\Delta H/RT + \Delta S/R \quad (3)$$

$$\ln(K_2/K_1) = (1/T_1 - 1/T_2)\Delta H/R \quad (4)$$

$$\Delta G = \Delta H - T\Delta S = -RT \ln K \quad (5)$$

where, $\Delta H$, $\Delta G$, and $\Delta S$ are enthalpy, free energy, and entropy change, respectively.


dx.doi.org/10.1021/jp2108279 | J. Phys. Chem. B 2012, 116, 2990−2998

Table 1. Dissociation Constants of Presequence Peptides with $Tim50_{IMS}$ Measured by Fluorescence Quenching

| | $K_D$ ($\mu$M) | | | |
|---|---|---|---|---|
| | 0.15 M NaCl | | 1.5 M NaCl | |
| | 25 °C | 35 °C | 25 °C | 35 °C |
| $Tim50_{IMS}$-pALDH | 3.16 ± 0.04 | 3.70 ± 0.05 | 13.94 ± 0.20 | 10.44 ± 0.17 |
| $Tim50_{IMS}$-pHsp60 | 7.79 ± 0.14 | 9.30 ± 0.18 | 24.43 ± 0.37 | 24.02 ± 0.35 |
| $Tim50_{IMS}$-pCoxIV | 4.98 ± 0.06 | 6.04 ± 0.07 | 17.89 ± 0.28 | 15.91 ± 0.21 |
| $Tim50_{IMS}$-pSyn | 83.76 ± 1.33 | 97.84 ± 1.68 | 188.35 ± 2.28 | 182.51 ± 2.45 |

**2.4. Fluorescence Resonance Energy Transfer.** A fluorescence resonance energy transfer experiment was performed at 25 °C. The excitation wavelength was set at 295 nm with a slit width of 5 nm, and the fluorescence emission spectra were scanned from 300 to 450 nm with a slit width of 5 nm. The concentration of $Tim50_{IMS}$ was 0.05 mg $mL^{-1}$ (1.6 $\mu$M) in 10 mM sodium phosphate buffer (pH 7.4) containing 0.15 M NaCl. According to Föster's nonradiative energy transfer theory,[21] the energy transfer effect is related not only to the distance between the acceptor and donor ($r$), but also to the critical energy transfer distance ($R_0$), and the equations used were

$$E = 1 - F/F_0 = (R_0)^6/((R_0)^6 + r^6) \quad (6)$$

$$(R_0)^6 = 8.8 \times 10^{-25} K^2 \phi N^{-4} J \quad (7)$$

$$\phi_x/\phi_{st} = (F_x/F_{st})(A_{st}/A_x) \quad (8)$$

$$J = (\sum F(\lambda)\varepsilon(\lambda)\lambda^4\Delta\lambda)/(\sum F(\lambda)\Delta\lambda) \quad (9)$$

where $R_0$ is the critical distance when the transfer efficiency ($E$) is 50%, $K^2$ is the spatial orientation factor of the dipole, $N$ is the refractive index of the medium, $\varphi$ is the fluorescence quantum yield of the donor, $A_x$ is the absorptance of the presequence peptide bound with 8-anilino-1-naphthalene-sulfonate (ANS) at 280 nm. The presequence peptides bound with ANS through covalent linking were prepared as follows. Briefly, ANS-Cl was prepared first, as described in a previous paper.[22] And then ANS-Cl and presequence peptides were covalently linked with a molar ratio of 1:1.[23] The presequence peptides bound with ANS were finally loaded onto a PD MiniTrap G-10 column (GE Healthcare). $J$ is the overlap integral of the fluorescence emission spectrum of the donor and the absorption spectrum of the acceptor, $F(\lambda)$ is the fluorescence intensity of $Tim50_{IMS}$ at wavelength $\lambda$, and $\varepsilon(\lambda)$ is the molar absorptivity of the acceptor at wavelength $\lambda$.

**2.5. Synchronous Fluorescence.** Synchronous fluorescence experiments were performed at 25 °C. The spectra were measured from 200 to 400 nm with 3 nm step and a slit width of 5 nm. $\Delta\lambda$ was set at 15 and 70 nm, respectively. The concentration of $Tim50_{IMS}$ was 0.05 mg $mL^{-1}$ (1.6 $\mu$M) in 10 mM sodium phosphate buffer (pH 7.4) containing 0.15 M NaCl. The spectra of samples were corrected by subtracting the corresponding spectra of buffers in the absence of protein.

**2.6. Micro-Raman Spectrum.** Micro-Raman spectra were recorded in the range of 400−1600 $cm^{-1}$ on a Renishaw Invia micro-Raman spectrometer (Britain). An exciting wavelength of 785 nm was provided by a laser source of 5.6 mW. The concentration of $Tim50_{IMS}$ was 20 mg $mL^{-1}$, and the molar ratio of $Tim50_{IMS}$ to presequence peptide was 1:1. The spectra were integrated 30 times to effectively eliminate the noise, and the standard deviation of signal was calculated by the Bessel equation.

The distribution of tyrosine residues in "buried" or "exposed" environments was calculated from the Raman data according the following equations:[24]

$$0.5N_b + 1.25N_e = I_{850}/I_{830} \quad (10)$$

$$N_b + N_e = 1 \quad (11)$$

where $N_b$ and $N_e$ are the mole fractions of buried and exposed tyrosine residues of $Tim50_{IMS}$, respectively.

## 3. RESULTS

**3.1. Interaction of $Tim50_{IMS}$ with Presequence Is Mainly an Electrostatic Interaction.** To estimate the interaction between the presequence peptide and $Tim50_{IMS}$, fluorescent quenching was used. As shown in Figure 2A, the Stern−Volmer plots were linear, and the slopes were increased with increasing temperature. From eq 1, $K_{SV}$ is equal to $K_q\tau_0$. The fluorescence lifetime of the biopolymer $\tau_0$ is $10^{-8}$ s;[25] therefore, the quenching constant $K_q$ was obtained from the slope $K_{SV}$ ($t$ = 25 °C, $K_q = 3.529 \times 10^{12}$ l $mol^{-1}$ $s^{-1}$, $t$ = 35 °C, $K_q = 3.892 \times 10^{12}$ l $mol^{-1}$ $s^{-1}$). However, the maximum scatter collision quenching constant of various quenchers with the biopolymer is $2.0 \times 10^{10}$ l $mol^{-1}$ $s^{-1}$,[26] and the rate constant of the protein quenching procedure initiated by the presequence peptide was greater than the $K_q$ of the scatter procedure, so the quenching was not initiated by dynamic collision but from compound formation, and eq 2 should be used. As shown in Figure 2B−E, the dissociation constants ($K_D$) estimated from the slopes (Table 1) showed that the binding of presequence peptides with $Tim50_{IMS}$ was strong compared with the binding of pSyn with $Tim50_{IMS}$ and it indicated that the binding of presequence peptide with $Tim50_{IMS}$ was specific.

To determine the interaction characteristics between $Tim50_{IMS}$ and the presequence peptide, eqs 4 and 5 were used. $\Delta H$, $\Delta S$, $\Delta G$ obtained from the equations (Table 2) showed that the interaction between $Tim50_{IMS}$ and presequence peptide was mainly an electrostatic interaction in 0.15

Table 2. Thermodynamics of $Tim50_{IMS}$−Presequence Peptide Association

| | $\Delta H$ (kJ $mol^{-1}$) | $\Delta S$ (J $K^{-1}$ $mol^{-1}$) | $\Delta G$ (kJ $mol^{-1}$) |
|---|---|---|---|
| 10 mM Sodium Phosphate Buffer (pH 7.4), 0.15 M NaCl | | | |
| $Tim50_{IMS}$−pALDH | −12 | 65 | −31 |
| $Tim50_{IMS}$−pHsp60 | −14 | 52 | −29 |
| $Tim50_{IMS}$−pCox IV | −15 | 52 | −30 |
| 10 mM Sodium Phosphate Buffer (pH 7.4), 1.5 M NaCl | | | |
| $Tim50_{IMS}$−pALDH | 22 | 167 | −28 |
| $Tim50_{IMS}$−pHsp60 | 1 | 93 | −26 |
| $Tim50_{IMS}$−pCox IV | 9 | 121 | −27 |


dx.doi.org/10.1021/jp2108279 | J. Phys. Chem. B 2012, 116, 2990−2998

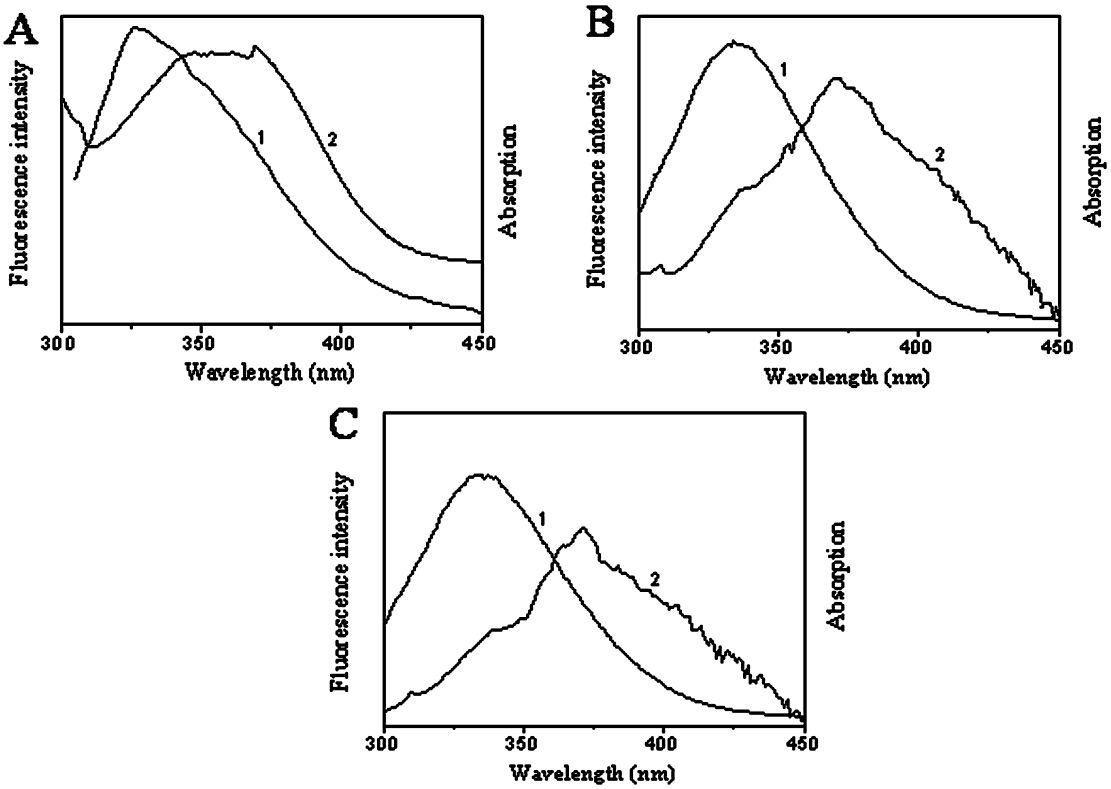


**Figure 3.** (A) Overlap of the fluorescence emission spectrum of $Tim50_{IMS}$ with the absorption spectrum of pCoxIV-ANS. (B) Overlap of the fluorescence emission spectrum of $Tim50_{IMS}$ with the absorption spectrum of pALDH-ANS. (C) Overlap of the fluorescence emission spectrum of $Tim50_{IMS}$ with the absorption spectrum of pHsp60-ANS. The fluorescence emission spectrum of $Tim50_{IMS}$ was performed at 25 °C with an excitation wavelength of 295 nm. The concentration of $Tim50_{IMS}$ was 1.6 $\mu$M in 10 mM sodium phosphate buffer (pH 7.4) with 0.15 M NaCl: (1) the fluorescence emission spectrum of $Tim50_{IMS}$; (2) the absorption spectrum of presequence-ANS.

M NaCl.[27] To further estimate whether there is hydrophobic interaction between $Tim50_{IMS}$ and presequence peptide, the same fluorescent quenching experiments were carried out in 1.5 M NaCl. The results from $K_D$, $\Delta H$, $\Delta S$, and $\Delta G$ showed that there is hydrophobic interaction in 1.5 M NaCl. Therefore, presequence peptides interact with $Tim50_{IMS}$ through both electrostatic interaction and hydrophobic interaction under physiologically relevant conditions, but mainly electrostatic interaction.

**3.2. Distance between $Tim50_{IMS}$ and Presequence Peptide.** Electronic excitation energy can be transferred nonradiatively between a fluorescent energy donor and a suitable energy acceptor over distances ranging from 1 to 10 nm. To calculate the distance between $Tim50_{IMS}$ and presequence peptide, eqs 6−9 were used. The overlap of the absorption spectrum of presequence peptide bound with ANS and the fluorescence emission spectrum of $Tim50_{IMS}$ were shown in Figure 3, and $J$ values were evaluated by integrating the spectra in Figure 3 for the range of $\lambda$ from 300 to 450 nm. Under these experimental conditions, we got $J$, $\varphi_x$, $R_0$, the energy transfer effect ($E$), and the distance ($r$) between $Tim50_{IMS}$ and presequence peptide (Table 3) using $K^2 = 2/3$, $N = 1.336$,[28] $\varphi_{st} = 0.13$.[29]

**3.3. Interaction of Presequence with $Tim50_{IMS}$ Influences the Environments of Tryptophan and Tyrosine Residues of $Tim50_{IMS}$.** To estimate the effect of presequence peptides on the environments of tryptophan and tyrosine residues of $Tim50_{IMS}$, synchronous fluorescence experiments were performed. The fluorescence spectra of $Tim50_{IMS}$ with excitation wavelengths of 275 nm and 295 nm

**Table 3. The Distances of Energy Donor and Acceptor Estimated by Fluorescence Resonance Energy Transfer**

| | $Tim50_{IMS}$-pALDH | $Tim50_{IMS}$-pHsp60 | $Tim50_{IMS}$-pCox IV |
|---|---|---|---|
| efficiency of energy transfer, $E$ | 0.470 | 0.165 | 0.308 |
| quantum yield, $\varphi_x$ | 0.189 | 0.188 | 0.189 |
| overlap integral, $J$ ($\times 10^{-15}$cm$^3$ M$^{-1}$) | 0.382 | 0.367 | 17.802 |
| critical distance, $R_0$ (nm) | 1.539 | 1.529 | 2.921 |
| distance, $r$ (nm) | 1.570 | 2.003 | 3.341 |

are shown in Figure 4B, which indicates that it was difficult to distinguish the fluorescence of tryptophan and tyrosine.[30] To assess the fluorescence changes of tryptophan and tyrosine of $Tim50_{IMS}$ due to presequence peptide, synchronous fluorescence spectra of tryptophan, tyrosine, and their mixture were recorded at 10, 20, 30, 40, 50, 60, 70, 80, 90, and 100 nm of $\Delta\lambda$, respectively (Figure 4A). As shown in Figure 4A, the profiles of fluorescence of tyrosine and the mixture of tryptophan and tyrosine almost overlapped when $\Delta\lambda$ was less than 20 nm, while the fluorescence of tryptophan and the mixture of tryptophan and tyrosine also almost overlapped when $\Delta\lambda$ was more than 60 nm. In order to distinguish the fluorescence of tyrosine and tryptophan of $Tim50_{IMS}$, the synchronous fluorescence experiments was performed at 15 nm and 70 nm of $\Delta\lambda$, respectively. As shown in Figure 4C, the fluorescences of tyrosine and tryptophan of $Tim50_{IMS}$ were obtained. The fluorescence quenching of $Tim50_{IMS}$ by presequence peptide at 15 and 70 nm of $\Delta\lambda$, respectively, showed that the interaction of


dx.doi.org/10.1021/jp2108279 | J. Phys. Chem. B 2012, 116, 2990−2998

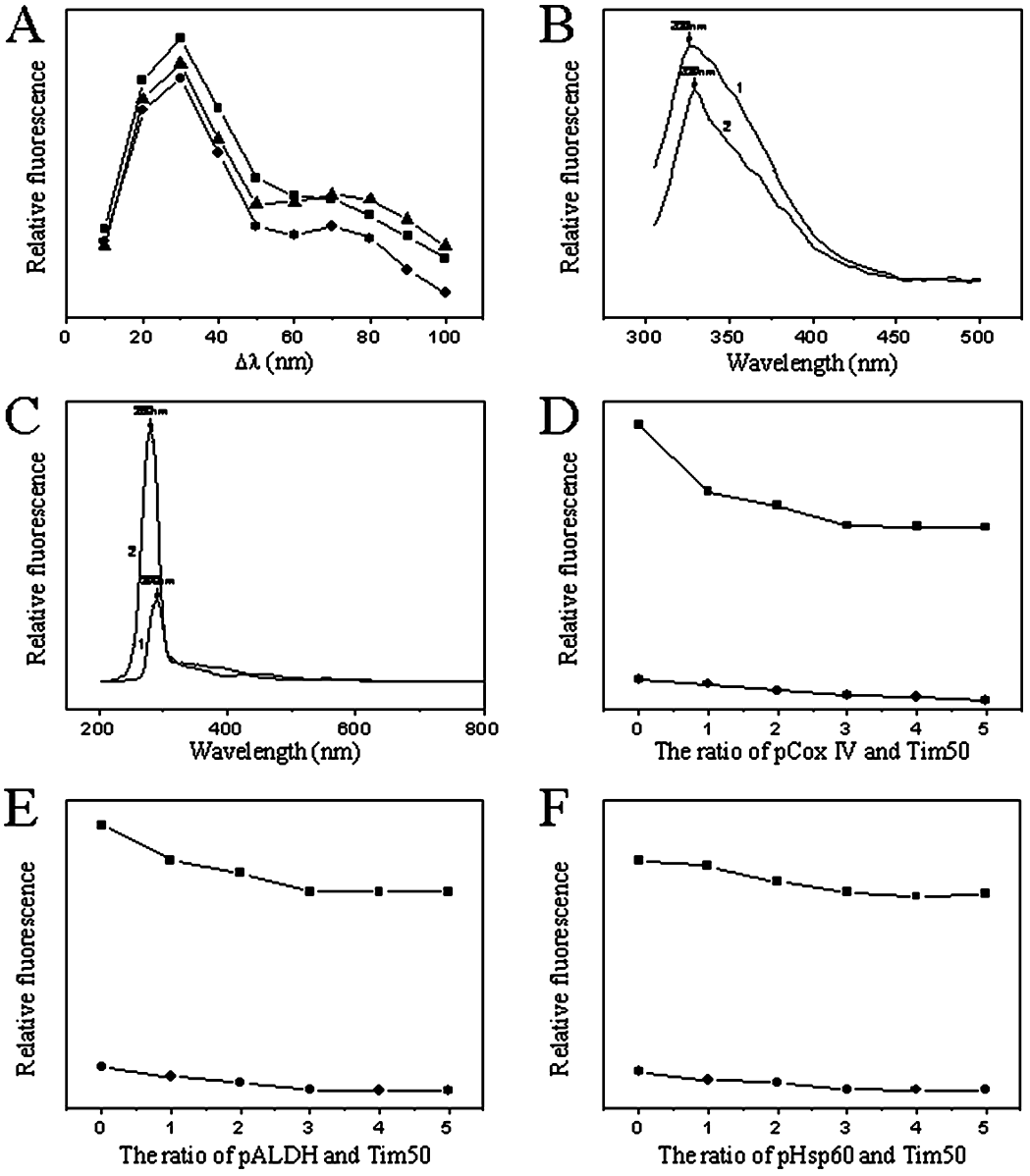


**Figure 4.** (A) The synchronous fluorescence of tryptophan, tyrosine, and their mixture at the different wavelength difference: (■) tryptophan; (●) tyrosine; (▲) the mixture of tryptophan and tyrosine with a molar ratio of tryptophan to tyrosine of 1:1. (B) The fluorescence emission spectrum of $Tim50_{IMS}$: (1) the fluorescence spectrum of tyrosine in $Tim50_{IMS}$ with an excitation wavelength of 275 nm; (2) the fluorescence spectrum of tryptophan in $Tim50_{IMS}$ with an excitation wavelength of 295 nm. (C) The synchronous fluorescence spectrum of $Tim50_{IMS}$: (1) the fluorescence spectrum of tyrosine in $Tim50_{IMS}$ with a wavelength difference of 15 nm; (2) the fluorescence spectrum of tryptophan in $Tim50_{IMS}$ with a wavelength difference of 70 nm. (D) The fluorescence quenching of $Tim50_{IMS}$ by pCoxIV with wavelength differences of 15 and 70 nm, respectively. (E) the fluorescence quenching of $Tim50_{IMS}$ by pALDH with wavelength differences of 15 and 70 nm, respectively. (F) the fluorescence quenching of $Tim50_{IMS}$ by pHsp60 with wavelength differences of 15 and 70 nm, respectively: (■) tryptophan; (●) tyrosine. The concentration of $Tim50_{IMS}$ was 1.6 $\mu$M in 10 mM sodium phosphate buffer (pH 7.4) containing 0.15 M NaCl.

presequence with $Tim50_{IMS}$ influenced the environments of tryptophan and tyrosine residues that became more hydrophobic, but mainly influenced tryptophan residues (Figure 4D–F). Furthermore, the tyrosine or tryptophan fluorescence quenching molar ratio of presequence peptide to $Tim50_{IMS}$ was less than 3.

**3.4. Presequence Peptide Induces a More Compact Conformation of $Tim50_{IMS}$.** Micro-Raman spectra have been widely used to investigate the structure of proteins.[31] To further obtain the details about the interaction of $Tim50_{IMS}$ with presequence peptide, micro-Raman spectra of $Tim50_{IMS}$ with and without presequence peptide were performed. The Raman spectra of $Tim50_{IMS}$ and the complex of $Tim50_{IMS}$ with presequence peptide are shown in Figure 5, which indicates many conformational details (Table 4). The bands located at 1240 to 1260 $cm^{-1}$ are useful to detect random coils.[32,33] The band at 1259 $cm^{-1}$ disappeared in lines c–e, indicating that the random coils of $Tim50_{IMS}$ were decreased due to the interaction of $Tim50_{IMS}$ with presequence peptide. The Raman spectrum in the region of 500–550 $cm^{-1}$ should be attributed to S–S vibration. The bands near 510, 525, and 540 $cm^{-1}$ due to the S–S stretching mode can be ascribed to gauche–gauche–gauche, gauche–gauche–trans, and trans–gauche–trans conformations of disulfide bonds, respectively.[34]


dx.doi.org/10.1021/jp2108279 | J. Phys. Chem. B 2012, 116, 2990–2998

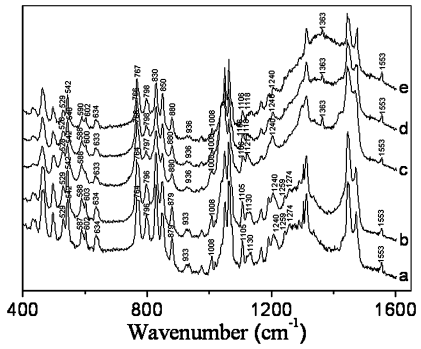


**Figure 5.** Micro-Raman spectra of $Tim50_{IMS}$ and the complex of $Tim50_{IMS}$ with presequence peptide. The Micro-Raman spectrum was performed at 25 °C with an excitation wavelength of 785 nm in the range of 400−1600 $cm^{-1}$. The molar ratio of $Tim50_{IMS}$ to presequence peptide was 1:1, and the concentration of $Tim50_{IMS}$ was 20 mg $mL^{-1}$. (a) $Tim50_{IMS}$; (b) $Tim50_{IMS}$ + pSyn; (c) $Tim50_{IMS}$ + pALDH; (d) $Tim50_{IMS}$ + pHsp60; (e) $Tim50_{IMS}$ + pCoxIV.

The bands at 528, 529 $cm^{-1}$ and 540, 542 $cm^{-1}$ indicated that the S−S stretching modes of $Tim50_{IMS}$ were gauche−gauche−trans, and trans−gauche−trans, respectively. The Raman bands at 630 to 670 $cm^{-1}$ and 700 to 745 $cm^{-1}$ can be ascribed to gauche and trans conformations of C−S, respectively,[35] and the band at 633, 634 $cm^{-1}$ revealed that the C−S conformation of $Tim50_{IMS}$ was gauche.

In protein, the side chain of tyrosine frequently binds with other residues through hydrogen bonds, and the changes of the hydrogen bonds can be used as a probe to detect the local tertiary structural changes. Among many tyrosine Raman bands, the doublet bands located near 830 and 850 $cm^{-1}$ are useful to determine the microenvironment around tyrosine side chains and the state of hydrogen bonding involving the tyrosine OH group.[36] The distribution of tyrosine residues in "buried" or "exposed" environments could be calculated according the eqs 10 and 11, and $N_e$ values for $Tim50_{IMS}$ and the complex of $Tim50_{IMS}$ with pSyn, pCox IV, pALDH, pHsp60 were 57.5%, 57.3%, 55.5%, 55.3%, 55.7%, respectively, revealing that the mole fraction of buried tyrosine residues of $Tim50_{IMS}$ were increased when $Tim50_{IMS}$ interacted with presequence peptides. The bands near 1360 $cm^{-1}$ are assigned to the tryptophan residues due to the Fermi resonance between one skeletal stretching fundamental and one or two combinations of the indole ring vibrations.[31,37] The spectra of the complex of $Tim50_{IMS}$ with presequence peptides at 1363 $cm^{-1}$ turned sharp compared to the spectrum of $Tim50_{IMS}$, indicating that some exposed tryptophan residues of $Tim50_{IMS}$ were changed into buried ones.

## 4. DISCUSSION

The fluorescence of tryptophan and tyrosine has been widely used to study the interaction between proteins and peptides. A valuable feature of intrinsic protein fluorescence is the high sensitivity of tryptophan to its local environment, which can frequently observe changes in emission spectra of tryptophan in response to protein conformational transitions, subunit association, substrate binding, or denaturation.[38,39] On the other hand, the emission fluorescence of tyrosine, which can undergo an excited-state ionization resulting in the loss of the proton on the aromatic hydroxyl group, is rather insensitive and often can be mistaken for tryptophan fluorescence.[40] The interaction of Tim50 with presequence is crucial for the TIM23 channel to transport the precursor protein across the mitochondrial inner membrane, but the interaction details between Tim50 and presequence peptide are not well-known. In the present study, we used fluorescence quenching, synchronous fluorescence, and micro-Raman spectra to study the interaction between $Tim50_{IMS}$ and presequence peptide, and the results showed that presequence peptides interact with $Tim50_{IMS}$ through both electrostatic interaction and hydrophobic interaction under physiologically relevant conditions, but mainly electrostatic interaction. Moreover, the interaction induces a compact conformation of $Tim50_{IMS}$, the interaction molar ratio of presequence peptide to $Tim50_{IMS}$ was less than 3, and the interaction mainly influenced the environments of tryptophan residues of $Tim50_{IMS}$, which became more hydrophobic.

TIM23 complex is the main entry gate for proteins of the matrix and the inner membrane. It has been intensively studied on the functions of yeast TIM23 complex.[41,42] Tim50, as a receptor, is essential for precursor proteins to be imported into the mitochondrial matrix.[43] It is known that precursors that carry an N-terminal, positively charged matrix-targeting signal

**Table 4. Assignment of the Main Bands in the Raman Spectra of $Tim50_{IMS}$[32−37]**

| assignments | Raman wavenumbers of $Tim50_{IMS}$ ($cm^{-1}$) | Raman wavenumbers of $Tim50_{IMS}$ with pSyn ($cm^{-1}$) | Raman wavenumbers of $Tim50_{IMS}$ with pCox IV ($cm^{-1}$) | Raman wavenumbers of $Tim50_{IMS}$ with pHsp60 ($cm^{-1}$) | Raman wavenumbers of $Tim50_{IMS}$ with pALDH ($cm^{-1}$) |
|---|---|---|---|---|---|
| $\alpha$-helix | 933 | 933 | 936 | 936 | 936 |
| $\beta$-sheet | 1240 | 1240 | 1240 | 1240 | 1240 |
| random coil | 1259 | 1259 | – | – | – |
| S−S | 529, 542 | 529, 542 | 529, 542 | 528, 540 | 528, 542 |
| C−S | 634 | 634 | 634 | 633 | 633 |
| C−N | 1105, 1130 | 1105, 1130 | 1106, 1118 | 1106, 1118 | 1106, 1121 |
| tyrosine | 830, 850 | 830, 850 | 830, 850 | 830, 850 | 830, 850 |
| tryptophan | 879, 1008 | 879, 1008 | 880, 1008, 1363 | 880, 1008, 1363 | 880, 1008, 1363 |
| amide II[a] | 1553 | 1553 | 1553 | 1553 | 1553 |
| amide III[b] | 1240, 1259, 1274 | 1240, 1259, 1274 | 1240 | 1240 | 1240 |
| amide IV[c] | 634, 764 | 634, 764 | 634, 767 | 633, 766 | 633, 766 |
| amide V[d] | 764, 796 | 764, 796 | 767, 798 | 766, 798 | 766, 797 |
| Amide VI[e] | 542, 587, 602 | 542, 588, 603 | 542, 590, 602 | 540, 588, 600 | 542, 588 |

[a]Amide II: C−N stretching, N−H deformation vibration. [b]Amide III: C−N stretching, N−H deformation vibration. [c]Amide IV: O=C−N deformation vibration. [d]Amide V: N−H deformation vibration. [e]Amide VI: C=O deformation vibration.


dx.doi.org/10.1021/jp2108279 | J. Phys. Chem. B 2012, 116, 2990−2998

(a presequence) are directed to the TIM23 complex,[10] and presequences selectively override the Tim50-induced closure and activate the TIM23 channel,[11] in which Tim50 promotes oligomerization and voltage-dependent closure of the channel. Many studies showed that the interaction between presequence peptide and Tim50 is hydrophobic interaction.[12−14] Qian et al.[15] recently reported the crystal structure of the IMS domain of yeast Tim50, and they found that Tim50 contains a large groove as putative binding site for presequences and the groove contains several exposed negatively charged residues, which may be ideally suited as a binding site for positively charged presequences/preproteins. In our case, we found that both electrostatic interaction and hydrophobic interaction exist between human $Tim50_{IMS}$ and presequence peptide, and the interaction is mainly through electrostatic interaction under physiologically relevant conditions.

Fluorescence resonance energy transfer has been widely used to study protein interaction. In our case, the excitation wavelength was set at 295 nm which excites the fluorescence of tryptophan. Therefore, the distances between presequence peptides and $Tim50_{IMS}$ estimated from fluorescence resonance energy transfer indicated the distance between a fluorescent energy donor tryptophan and an energy acceptor ANS, which indirectly revealed the interaction between presequence peptides and $Tim50_{IMS}$. The similarity of the amide acid sequence of human $Tim50_{IMS}$ with yeast $Tim50_{IMS}$ is 35.7%,[9] and there are four tryptophan residues in human $Tim50_{IMS}$. Qian et al.[15] reported that yeast Tim50 contains a protruding $\beta$-hairpin, which is the largest conserved area on the molecular surface, and the C-terminal region of Tim50 (residues 362−476) is not essential for biogenesis of Tim50. Compared with the crystal structure of yeast $Tim50_{IMS}$, the residues Trp-163 and Trp-169 in human $Tim50_{IMS}$ should be in the protruding $\beta$-hairpin (B2, B3), Trp-267 near the binding groove in the random coil locates between B9 and A3, and Trp-347 locates in the C-terminal region of Tim50, which is not essential for biogenesis of Tim50. So we speculated that the interaction between human $Tim50_{IMS}$ and presequence peptides may influence the environment of residue Trp-267.

Micro-Raman spectroscopy of the protein is a reliable tool to monitor the changes in protein structure and microenvironment of side chains.[31−33] In Raman spectra of proteins, the region of 500−550 $cm^{-1}$ should be attributed to S−S vibration.[32−35] The bands near 510, 525, and 540 $cm^{-1}$ due to the S−S stretching mode can be ascribed to gauche−gauche−gauche, gauche−gauche−trans, and trans−gauche−trans conformations of disulfide bonds, respectively.[34] Yeast $Tim50_{IMS}$ contains one cysteine residue Cys-268, whereas human $Tim50_{IMS}$ contains three cysteine residues Cys-133, Cys-236, and Cys-249. In Raman spectra of $Tim50_{IMS}$/$Tim50_{IMS}$ with presequence, the bands at 528/529 $cm^{-1}$ and 540/542 $cm^{-1}$ should indicate that the S−S stretching modes of human $Tim50_{IMS}$ were gauche−gauche−trans and trans−gauche−trans, respectively. Considering the fact that $Tim50_{IMS}$ is a monomer,[15,17] the conclusion that there is a disulfide bond in human $Tim50_{IMS}$ intramolecule can be deduced.

In Raman spectra, the spectra were integrated 30 times to effectively eliminate the noise, and the standard deviation of signal was calculated by the Bessel equation. From the standard deviation of signal, we got the $N_e$ of tyrosine residues for $Tim50_{IMS}$ with and without presequence peptide in the ranges of 55.2−56.1% and 56.9−58.5%, respectively, indicating that the interaction of presequence peptide with $Tim50_{IMS}$ influenced the environments of tyrosine residues, which became more hydrophobic. The spectra of the complex of $Tim50_{IMS}$ with presequence peptide at 1363 $cm^{-1}$ turned sharp compared to the spectrum of $Tim50_{IMS}$, indicating that some exposed tryptophan residues of $Tim50_{IMS}$ were changed into buried ones. These results were consistent with the results measured by synchronous fluorescence.

## 5. CONCLUSION

Tim50 as a receptor is crucial for transporting the precursor protein across the mitochondrial inner membrane in TIM23 complex, and the dysfunction of Tim50 induces cell apoptosis and several diseases. Although the micro-Raman and fluorescence spectra have been used to study conformational changes of proteins, the interactions of proteins with peptides studied by these methods have been seldom reported. In our manuscript, we have successfully investigated the interaction of $Tim50_{IMS}$ protein with presequence peptide using micro-Raman and fluorescence spectra. The fluorescence quenching revealed that presequence peptides interact with $Tim50_{IMS}$ through both electrostatic interaction and hydrophobic interaction under physiologically relevant conditions, but mainly electrostatic interaction. The fluorescence resonance energy transfer indicated the distances between presequence peptides and $Tim50_{IMS}$. Synchronous fluorescence showed that the interaction of presequence peptides with $Tim50_{IMS}$ mainly influenced the environments of tryptophan residues of $Tim50_{IMS}$, and the tyrosine or tryptophan fluorescence quenching molar ratio of presequence peptide to $Tim50_{IMS}$ was less than 3. Micro-Raman spectra showed that presequence peptides induce a more compact conformation of $Tim50_{IMS}$.

## AUTHOR INFORMATION

### Corresponding Author

*Address: The Key Laboratory of Bioactive Materials, Ministry of Education, School of Physics Science, Nankai University, Tianjin 300071, P. R. China. Tel: +86-22-2350-6973; fax: +86-22-2350-6973; e-mail: shujieli@nankai.edu.cn.

### Notes

The authors declare no competing financial interest.

## ACKNOWLEDGMENTS

This work was supported by National Natural Science Foundation of China (No. 30970579).

## REFERENCES

(1) Ryan, M. T.; Wagner, R.; Pfanner, N. *Int. J. Biochem. Cell Biol.* **2000**, *32*, 13−21.
(2) Gabriel, K.; Buchanan, S. K.; Lithgow, T. *Trends Biochem. Sci.* **2001**, *26*, 36−40.
(3) Pfanner, N.; Wiedemann, N.; Meisinger, C.; Lithgow, T. *Nat. Struct. Mol. Biol.* **2004**, *11*, 1044−1048.
(4) Endo, T.; Yamano, K.; Kawano, S. *Biochim. Biophys. Acta* **2011**, *1808*, 955−970.
(5) Endo, T.; Yamano, K. *Biochim. Biophys. Acta* **2010**, *1803*, 706−714.
(6) Schmidt, O.; Pfanner, N.; Meisinger, C. *Nat. Rev. Mol. Cell Biol* **2010**, *11*, 655−667.
(7) Mokranjac, D.; Neupert, W. *Biochim. Biophys. Acta* **2010**, *1797*, 1045−1054.
(8) von Heijne, G. *EMBO J.* **1986**, *5*, 1335−1342.
(9) Yamamoto, H.; Esaki, M.; Kanamori, T.; Tamura, Y.; Nishikawa, S.; Endo, T. *Cell* **2002**, *111*, 519−528.

(10) Mokranjac, D.; Sichting, M.; Popov-Celeketic, D.; Mapa, K.; Gevorkyan-Airapetov, L.; Zohary, K.; Hell, K.; Azem, A.; Neupert, W. *Mol. Biol. Cell* **2009**, *20*, 1400−1407.
(11) Meinecke, M.; Wagner, R.; Kovermann, P.; Guiard, B.; Mick, D. U.; Hutu, D. P.; Voos, W.; Truscott, K. N.; Chacinska, A.; Pfanner, N.; Rehling, P. *Science* **2006**, *312*, 1523−1526.
(12) Yamamoto, H.; Itoh, N.; Kawano, S.; Yatsukawa, Y.; Momose, T.; Makio, T.; Matsunaga, M.; Yokota, M.; Esaki, M.; Shodai, T.; Kohda, D.; Hobbs, A. E.; Jensen, R. E.; Endo, T. *Proc. Natl. Acad. Sci. U.S.A.* **2011**, *108*, 91−96.
(13) Marom, M.; Dayan, D.; Demishtein-Zohary, K.; Mokranjac, D.; Neupert, W.; Azem, A. *J. Biol. Chem.* **2011**, *286*, 43809−43815.
(14) Schulz, C.; Lytovchenko, O.; Melin, J.; Chacinska, A.; Guiard, B.; Neumann, P.; Ficner, R.; Jahn, O.; Schmidt, B.; Rehling, P. *J. Cell Biol.* **2011**, *195*, 643−656.
(15) Qian, X.; Gebert, M.; Höpker, J.; Yan, M.; Li, J.; Wiedemann, N.; van der Laan, M.; Pfanner, N.; Sha, B. *J. Mol. Biol.* **2011**, *411*, 513−519.
(16) Guo, Y.; Cheong, N.; Zhang, Z.; De Rose, R.; Deng, Y.; Farber, S. A.; Fernandes-Alnemri, T.; Alnemri, E. S. *J. Biol. Chem.* **2004**, *279*, 24813−24825.
(17) Zhang, Y.; Xu, Y.; Zhao, Q.; Ji, Z.; Li, Q.; Li, S. J. *Protein Expression Purif.* **2011**, *80*, 130−137.
(18) Pace, C. N.; Vajdos, F.; Fee, L.; Grimsley, G.; Gray, T. *Protein Sci.* **1995**, *4*, 2411−2423.
(19) Truscott, K. N.; Kovermann, P.; Geissler, A.; Merlin, A.; Meijer, M.; Driessen, A. J.; Rassow, J.; Pfanner, N.; Wagner, R. *Nat. Struct. Biol.* **2001**, *12*, 1074−1082.
(20) Eftink, M. R.; Ghiron, C. A. *Anal. Biochem.* **1981**, *114*, 199−227.
(21) Sklar, L. A.; Hudson, B. S.; Simoni, R. D. *Biochemistry* **1977**, *16*, 5100−5108.
(22) Muramoto, K.; Kamiya, H. *Agric. Biol. Chem.* **1984**, *48*, 2695−2699.
(23) Gray, W. R. *Methods in Enzymology*; Academic Press Inc: New York, 1967; p 139.
(24) Craig, W. S.; Gaber, B. R. *J. Am. Chem. Soc.* **1977**, *99*, 4130−4134.
(25) Lakowicz, J. R.; Weber, G. *Biochemistry* **1973**, *12*, 4161−4170.
(26) Ware, W. R. *J. Phys. Chem.* **1962**, *66*, 455−458.
(27) Ross, D. P.; Sabramanian, S. *Biochemistry* **1981**, *20*, 3096−3102.
(28) Cyril, L.; Earl, J. K.; Sperry, W. M. *Biochemists Handbook*; E & F.N. Spon: London, 1961; p 83.
(29) Burstein, E. A.; Vedenkina, N. S.; Ivkova, M. N. *Photochem. Photobiol.* **1973**, *18*, 263−279.
(30) Lakowica, J. R. *Principles of Fluorescent Spectroscopy*; Plenum Press: New York, 1982; pp 257−301.
(31) Shou, J. J.; Zeng, G.; Zhang, Y. H.; Lu, G. Q. *J. Phys. Chem. B* **2009**, *113*, 9633−9635.
(32) Carey, P. R. *Biochemical Applications of Raman and Resonance Raman Spectroscopies. A Subsidiary of Harcourt Brace Jovanovich*; Academic Press: New York, 1982; pp 71−96.
(33) Bandekar, J.; Krimm, S. *J. Biopolymers* **1980**, *19*, 31−36.
(34) Tu, A. T. *Spectroscopy of Biological System*; John Wiley and Sons: New York, 1986; p 47.
(35) Lord, R. C.; Yu, N. T. *J. Mol. Biol.* **1970**, *50*, 509−524.
(36) McHale, J. L. *J. Raman Spectrosc.* **1982**, *13*, 21−24.
(37) Chen, M. C.; Lord, R. C.; Mendelso, R. *J. Am. Chem. Soc.* **1974**, *96*, 3038−3042.
(38) Jones, B. E.; Beechem, J. M.; Matthews, C. R. *Biochemistry* **1995**, *34*, 1867−1877.
(39) Eftink, M. R. *Biophys. J.* **1994**, *66*, 482−501.
(40) Willis, K. J.; Szabo, A. G. *J. Phys. Chem.* **1991**, *95*, 1585−1589.
(41) Bauer, M. F.; Sirrenberg, C.; Neupert, W.; Brunner, M. *Cell* **1996**, *87*, 33−41.
(42) Chacinska; Lind, M.; Frazier, A. E.; Dudek, J.; Meisinger, C.; Geissler, A.; Sickman, A.; Meyer, H. E.; Truscott, K. N.; Guiard, B.; Pfanner, N.; Rehling, P. *Cell* **2005**, *120*, 817−829.
(43) Geissler; Chacinska, A.; Truscott, K. N.; Wiedemann, N.; Brandner, K.; Sickmann, A.; Meyer, H. E.; Meisinger, C.; Pfanner, N.; Rehling, P. *Cell* **2002**, *111*, 507−518.